

Shared role of the pRB-related p130 and p107 proteins in limb development

David Cobrinik,^{1,2} Myung-Ho Lee,³ Gregory Hannon,⁴ George Mulligan,⁶ Roderick T. Bronson,⁵ Nicholas Dyson,³ Ed Harlow,³ David Beach,⁴ Robert A. Weinberg,^{1,7} and Tyler Jacks^{6,7,8}

¹Whitehead Institute for Biomedical Research, Cambridge, Massachusetts 02142 USA; ²Columbia University College of Physicians and Surgeons, New York, New York 10032 USA; ³Massachusetts General Hospital Cancer Center, Charlestown, Massachusetts 02129 USA; ⁴Howard Hughes Medical Institute, Cold Spring Harbor Laboratory, Cold Spring Harbor, New York 11724 USA; ⁵Tufts University School of Medicine, Boston, Massachusetts 02111 USA; ⁶Howard Hughes Medical Institute and Center for Cancer Research and ⁷Department of Biology, Massachusetts Institute of Technology, Cambridge, Massachusetts 02142 USA

The p130 protein shares extensive sequence similarity with pRB, the product of the retinoblastoma gene, and is a major E2F-associated protein in quiescent cells. To investigate its biological function, we have mutated p130 via gene targeting in the mouse. Homozygous mutation of p130 had little discernible effect on development or on the growth of mouse embryo fibroblasts in culture. Much of the E2F activity that normally associates with p130 in serum-starved mouse embryo fibroblasts associated instead with the highly related p107 protein. To determine whether p130 and p107 have overlapping biological roles, we produced mice having simultaneous inactivation of the p130 and p107 genes. Such mice exhibited deregulated chondrocyte growth, defective endochondral bone development, shortened limbs, and neonatal lethality. These findings indicate that p130 and p107 play an important role in limb development through their abilities to control chondrocyte proliferation. Thus, in certain settings p107 and p130 perform growth-regulatory functions that are not fulfilled by pRB.

[Key Words: p130; p107; RB family; chondrocyte; cartilage development; gene targeting]

Received April 22, 1996; accepted May 16, 1996.

pRB is an important regulator of cell cycle progression. Through its interactions with E2F transcription factors and other cellular proteins, pRB inhibits the G₁-to-S-phase cell cycle transition. The growth-inhibitory action of pRB is negated in late G₁ through its phosphorylation by cyclin-dependent kinases (cdks), specifically cyclin D/cdk4 and cyclin E/cdk2; thereafter, pRB remains in a phosphorylated, inactive configuration throughout S and G₂. The biological importance of cell growth regulation by pRB is highlighted by the widespread mutation of this gene in human cancer and by the developmental abnormalities that occur in pRB-deficient mice (for review, see Weinberg 1995).

pRB is a member of a protein family that also includes p107 and p130 (Ewen et al. 1991; Hannon et al. 1993; Li et al. 1993; Mayol et al. 1993). The three proteins share extensive structural similarity and are most highly related in a bipartite binding domain through which each interacts with DNA tumor virus oncoproteins and cellular targets such as E2Fs (DeCaprio et al. 1988; Whyte et al. 1988; Dyson et al. 1989; Hu et al. 1990; Huang et al.

1990; Kaelin et al. 1990; Ewen et al. 1991; Cobrinik et al. 1993; Hannon et al. 1993; Li et al. 1993; Zhu 1993; Vairo et al. 1995). However, p107 and p130 are more similar to each other than to pRB and have distinct biochemical functions.

p107 and p130 bind and inhibit the cyclin E/cdk2 and cyclin A/cdk2 kinases through a domain that is not present in pRB but is similar to the cdk2 binding domains of the p21, p27, and p57 cdk inhibitors (Ewen et al. 1991, 1992; Faha et al. 1992; Zhu 1993; Smith and Nevins 1995; Zhu et al. 1993, 1995a,b). p107 and p130 also bind and inhibit *trans*-activation by E2F family members and other transcription factors that are different from those controlled by pRB (Lees et al. 1993; Beijersbergen et al. 1994a,b; Ginsberg et al. 1994; Gu et al. 1994; Hoang et al. 1995; Sardet et al. 1995; Vairo et al. 1995). Through these distinct binding specificities, p107 and p130 may inhibit the expression of a class of genes distinct from those controlled by pRB (Dagnino et al. 1995). p107 and p130 are also regulated by cyclins and cdks in ways that differ substantially from the regulation of pRB (Cobrinik et al. 1993; Beijersbergen et al. 1995; Zhu et al. 1995b). Thus, while each of the pRB family members is expressed in a wide variety of cell types and can inhibit cell proliferation (Huang et al. 1988; Zhu et al. 1993; Claudio et al. 1994; Vairo et al. 1995), p107 and p130

²Present address: Columbia University College of Physicians and Surgeons, New York, New York 10032 USA.

⁸Corresponding author.

appear to function in growth-signaling pathways distinct from those involving pRB.

Recent evidence has suggested functions for p107 and p130 in DNA damage-induced growth arrest and in tumor suppression. These roles have been inferred from the deregulated growth of cells in which pRB, p107, and p130 have been functionally inactivated by DNA tumor virus oncoproteins when compared to the growth of cells that lack only pRB function (Slebos et al. 1994; Christensen and Imperiale 1995; Zalvide and DeCaprio 1995). A tumor suppressor role for p107 and p130 was suggested further by the potent oncogenicity of E2F-4 transcription factor mutants that are resistant to p107 [and probably p130] binding (Beijersbergen et al. 1994b; Ginsberg et al. 1994).

The production and analysis of pRB-deficient embryos and chimeric mice has revealed a critical role for pRB in the regulation of neuronal and lens fiber cell proliferation during embryogenesis and in the regulation of pituitary and adrenal cell proliferation during later development (Clarke et al. 1992; Jacks et al. 1992; Lee et al. 1992; Maandag et al. 1994; Morgenbesser et al. 1994; Williams et al. 1994). However, the aberrations resulting from pRB deficiency were surprisingly limited, given its perceived importance to cell cycle regulation. Through less direct experiments, p130 and p107 have also been implicated in development. In particular, the association of p130 with E2F transcription factors was found to be enhanced during muscle differentiation *in vitro*, and p107 expression was induced in differentiated pRB-deficient myocytes (Schneider et al. 1994; Shin et al. 1995). Together, these observations suggested that cell growth control exerted by p107 and p130 might have important developmental consequences.

To investigate the functions of these two proteins, we have produced mice with targeted mutations in the *p107* and *p130* genes. As described in Lee et al. (this issue), mice are largely unaffected by homozygous inactivation of their *p107* gene. We demonstrate here that mice homozygous for a null *p130* allele also exhibit minimal developmental consequences, whereas homozygosity for null alleles of both *p107* and *p130* elicits a cell type-specific defect in growth control and reveals a shared role of p107 and p130 in limb development.

Results

Production of mice with null p130 alleles

A *p130* gene targeting vector was constructed in which sequences in a 5' proximal exon of the *p130* gene were replaced by the neomycin resistance gene (*neo*) in the opposite transcriptional orientation to that of *p130* (see Materials and methods). This vector contained 3.2 and 4.8 kb of mouse 129/Sv genomic DNA flanking *neo*, as well as a *thymidine kinase* (*tk*) marker gene for negative selection (Fig. 1A). Homologous recombination of the *p130* targeting vector with mouse genomic DNA was predicted to produce a null *p130* allele, in which the

mouse *p130* codon corresponding to human *p130* amino acid 105 was joined to the *neo* cassette causing the *p130* coding sequence to be interrupted by an in-frame termination codon after residue 106.

The *p130* gene targeting vector was introduced into strain 129/Sv D3 embryonic stem (ES) cells by electroporation, and these cells were subjected to positive and negative selection with G418 and gancyclovir (Mansour et al. 1988). Cell clones in which the targeting vector had undergone homologous recombination with the endogenous *p130* gene on both sides of the *neo* cassette (about one-third of the surviving colonies) were identified by Southern blotting (Fig. 1B; data not shown). Two properly targeted ES cell clones were injected into C57BL/6 blastocysts to generate chimeras that transmitted the mutant *p130* allele through the germ line.

Mice heterozygous for the mutant *p130* allele appeared normal and exhibited no increase in morbidity or mortality when observed until 16 months of age. These mice were used in an F₁ cross to determine whether p130 was required for embryonic development. Of the 61 mice born in the first nine F₂ litters, 14 (23%) were homozygous for the mutant allele (Table 1A). Because *p130* homozygous mutants were generated in numbers that approximated the predicted Mendelian frequency, we concluded that this mutation had no substantial effect on prenatal viability. Homozygous *p130* mutant mice were of normal size and appearance at birth, displayed no detected histologic abnormalities at birth and at 2 months of age, and reproduced normally.

To determine whether the disrupted *p130* gene functioned as a null allele, cells derived from *p130* homozygous mutant mice were tested for p130 expression. The amount of p130 mRNA was reduced more than five-fold in liver cells from *p130* homozygous mutant mice as compared to wild type mice (data not shown). To examine the effect of the mutation on p130 protein levels, mouse embryonic fibroblasts (MEFs) were prepared, and cell extracts were immunoprecipitated using antiserum directed against p130 carboxy-terminal sequences. The presence of p130 in the immunoprecipitate was assessed by Western blot analysis with the same antiserum. Although p130 was readily detected in wild-type cells, none was observed in homozygous cells and intermediate levels were present in heterozygous cells (Fig. 1C). p130 was also undetectable in liver extracts from 6-month-old *p130* homozygous mutant mice but was readily detected in liver from wild-type mice (data not shown). These results indicated that the mutant *p130* allele is a null, and we therefore refer to this allele hereafter as *p130*^{-/-}.

Effect of p130 loss on cell growth and E2F complex formation in vitro

Effects of p130 loss on the *in vitro* growth of MEFs were also assessed. Consistent with the normal appearance of *p130*^{-/-} mice, MEFs derived from such mice showed normal distribution in the various cell cycle phases dur-

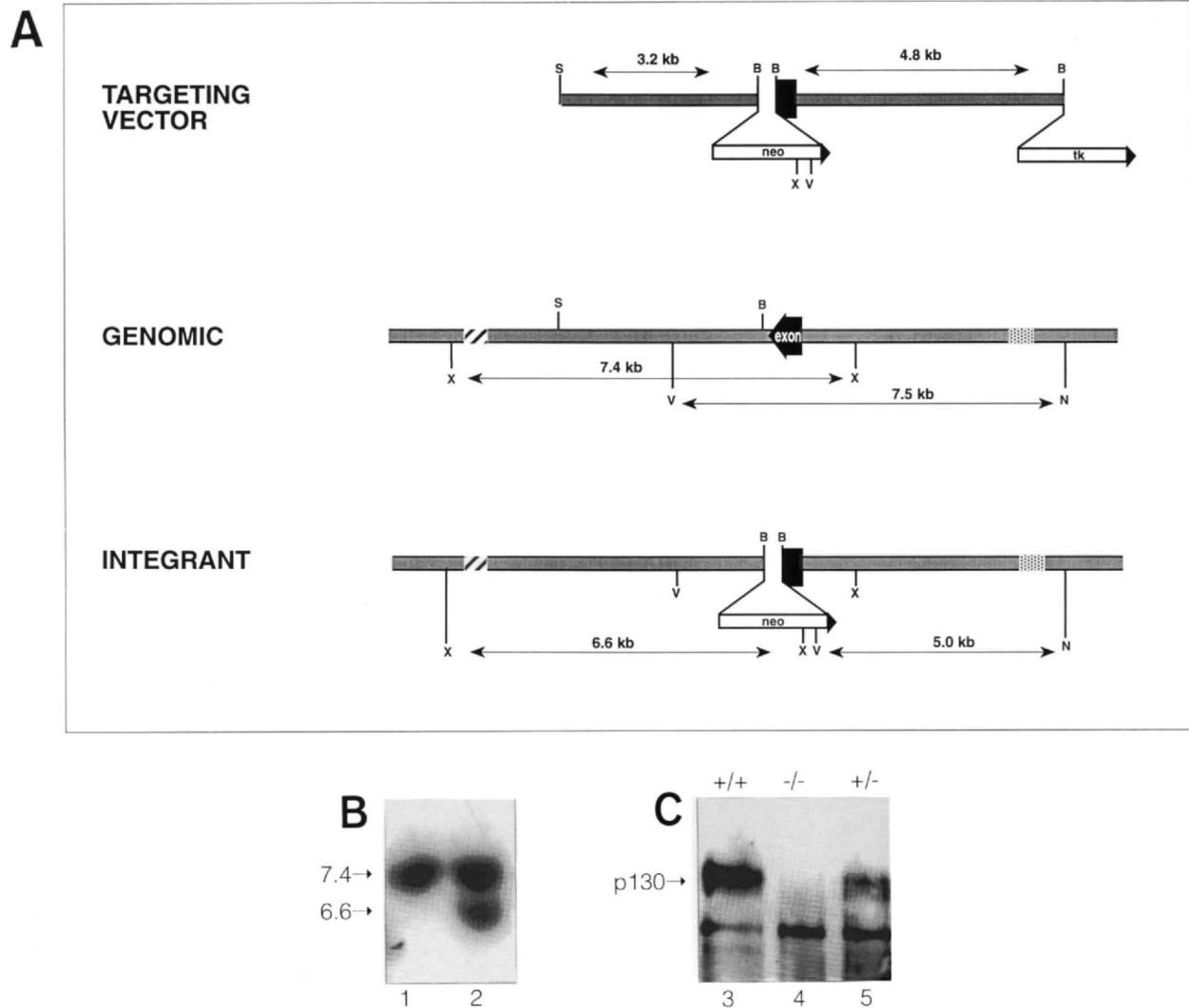


Figure 1. Targeted disruption of *p130*. (A) Targeted disruption strategy. The pPNT-*p130* gene targeting vector (top) is aligned with genomic intron (shaded) and exon (solid) DNA (middle). *neo* and *tk* genes are represented by open bars. Arrowheads indicate direction of transcription. The homologously recombined integrant (below) has a 6.6-kb *Bst*XI fragment compared to 7.4-kb *Bst*XI fragment in parental 129/Sv DNA using a probe represented by the hatched box, and a 5.0-kb *EcoRV/NotI* fragment compared to a 7.5-kb fragment in parental DNA using a probe represented by the stippled box. (B) Southern blot analysis of ES cell DNA derived from parental 129/Sv cells (lane 1) and a homologous recombinant (lane 2). (C) Immunoprecipitation and Western blot detection of p130 in *p130*^{+/+} (lane 3), *p130*^{-/-} (lane 4), and *p130*^{+/-} (lane 5) MEFs.

ing exponential growth as determined by FACS analysis (Fig. 2A). Moreover, they required the normal time to progress from G₀ to S phase following serum starvation and restimulation (Fig. 2B). This behavior was similar to that of *p107*^{-/-} fibroblasts (Lee et al., this issue), but it contrasted with that of *Rb*^{-/-} fibroblasts, which have a decreased G₀/G₁ population in growing cells and a shortened G₀-to-S transit time (Almasan et al. 1995; Lukas et al. 1995; Herrera et al. 1996)

The lack of effect of p130 loss on MEF growth was unexpected, as p130 is a major component of E2F complexes in these cells during the G₀ phase of the cell cycle (Cobrinik et al. 1993). To address whether the E2Fs that normally bind to p130 interacted with other pRB family proteins in *p130* homozygous mutant cells, we per-

formed a gel mobility shift analysis. As found previously, DNA-binding activities corresponding to free and complexed forms of E2F were detected in serum-starved wild-type cells (Fig. 2C, lane 1). Moreover, antibody directed against p130 supershifted the majority of the complexed E2F, whereas antibody directed against p107 supershifted only a minority of these complexes (Fig. 2C, lanes 1–3).

In *p130*^{-/-} cells, both free and complexed E2F were also detected (Fig. 2C, lane 4). However, in these cells the p107 antibody supershifted all of the complexed E2F, and the level of p107-associated E2F was increased (Fig. 2C, cf. the anti-p107-dependent supershift in lanes 2 and 5). The p130 antibody failed to supershift such complexes but did disrupt a portion of these complexes (lane 6),

Table 1. Genotype frequencies of mouse cross progeny

A. $p130^{+/-} \times p130^{+/-}$									
<i>p130</i>	+/+	+/-	-/-						
	9	38	14						
Percent	15.8	62.3	23.0						
Expected percent	25.0	50.0	25.0						
B. $p107^{+/-};p130^{+/-} \times p107^{+/-};p130^{+/-}$									
<i>p130</i>	+/+	+/-	-/-	+/+	+/-	-/-	+/+	+/-	-/-
<i>p107</i>	+/+	+/-	-/-	+/+	+/-	-/-	+/+	+/-	-/-
	18	20	10	35	40	20	16	35	3 (dec) ^a
Percent	9.1	10.2	5.1	17.8	20.3	10.2	8.1	17.8	1.5
Expected percent	6.2	12.5	6.2	12.5	25	12.5	6.2	12.5	6.2
C. $p107^{+/-};p130^{-/-} \times p107^{+/-};p130^{+/-}$									
<i>p130</i>	+/+	+/-	-/-	+/+	+/-	-/-			
<i>p107</i>	+/+	+/-	-/-	+/+	+/-	-/-			
	18	14	16	13	17	16			
Percent	19.1	14.9	17.0	13.8	18.1	17			
Expected percent	12.5	25	12.5	12.5	25	12.5			

Parental genotypes are indicated (A–C). Expected percent assumes Mendelian inheritance of wild-type and null alleles.
^a(dec) Deceased.

presumably owing to its weak cross-reactivity with p107 (D. Cobrinik, unpubl.). These findings indicated that p107 replaced p130 as the major E2F-associated species in $p130^{-/-}$ MEFs, which is consistent with the demonstrated abilities of both of these proteins to bind to E2F-4 (Vairo et al. 1995).

Significantly, p107 did not completely compensate for

the absence of p130 in the binding of E2Fs in $p130^{-/-}$ cells, as a greater proportion of E2F was in the free form in the mutant cells (Fig. 2C, cf. lanes 1 and 4). The failure of p107 to fully substitute for the E2F binding of p130 may be attributable to insufficient p107 levels in G_0 (see Cobrinik et al. 1993) or to insufficient affinity of p107 for certain E2F species that are normally bound by p130 (Hi-

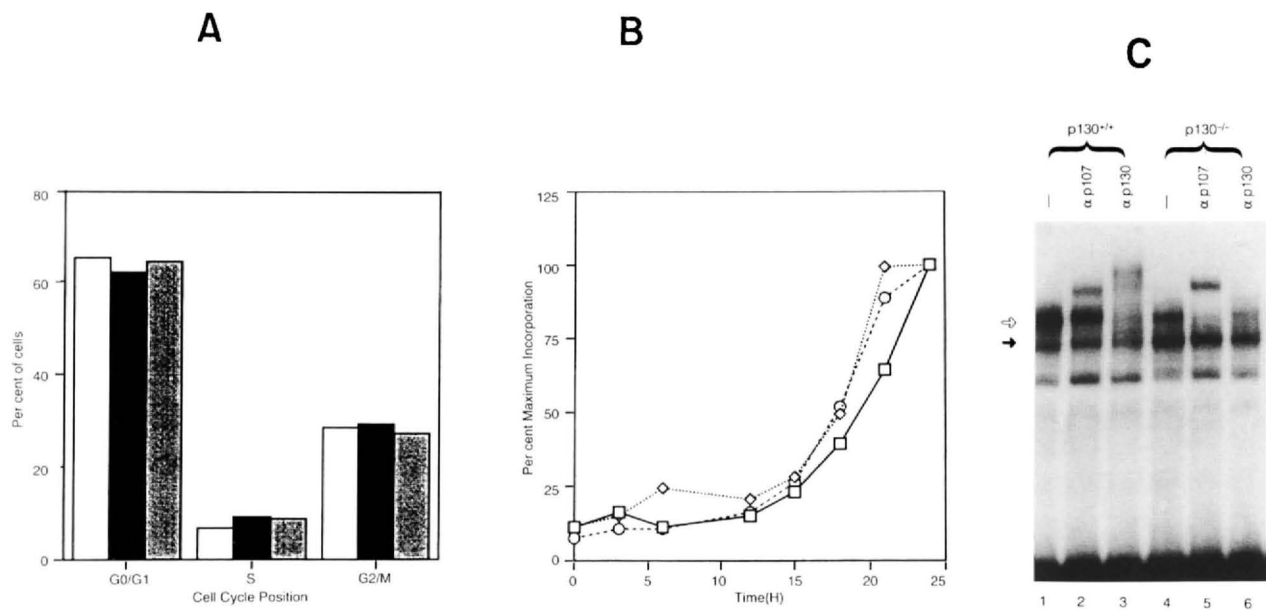


Figure 2. Characterization of cells lacking p130. (A) Cell cycle position of exponentially growing $p130^{+/+}$ (open bar), $p130^{+/-}$ (solid bar), and $p130^{-/-}$ (shaded bar) MEFs as determined by FACS analysis. (B) Thymidine incorporation of $p130^{+/+}$ (□), $p130^{+/-}$ (○), and $p130^{-/-}$ (◇) MEFs following serum starvation and restimulation. (C) Gel shift analysis of E2F complexes in $p130^{+/+}$ (lanes 1–3) and $p130^{-/-}$ (lanes 4–6). MEF extracts incubated with antibody directed against p107 (lanes 2,5) or p130 (lanes 3,6). The dark and light arrows indicate the positions of the free and complexed forms of E2F, respectively.

jmans et al. 1995). In either case, the increase in free E2F as detected in these gel shift analyses did not appear to influence the growth characteristics of the MEF preparations.

Viability and growth of mice with null p130 and p107 alleles

The similarity in structure and biochemical function of the p107 and p130 proteins suggested a possible overlap in biological function. This in turn provided one explanation of why deficiency of one or the other gene resulted in no obvious effects on mouse development. To address this possibility, we bred mice lacking functional alleles of both *p107* and *p130*.

p107^{+/-};*p130*^{+/-} compound heterozygotes produced in initial matings appeared normal and were mated to one another. In the first 28 litters of this cross, 194 neonates were alive at postnatal day 0.5. Of these, eight of the nine possible genotypes were present in numbers consistent with Mendelian inheritance of the wild-type and null *p107* and *p130* alleles (Table 1B). However, no live double homozygous *p107*^{-/-};*p130*^{-/-} neonates were detected, and dead *p107*^{-/-};*p130*^{-/-} neonates [3] were detected at below the expected frequency. This result suggested that a large proportion of such embryos either failed to develop in utero or died shortly after birth with defects that caused them to be consumed rapidly by their mothers.

To determine why fewer than the expected number of *p107*^{-/-};*p130*^{-/-} neonates were seen, we assessed the viability of *p107*^{-/-};*p130*^{-/-} embryos at 18.0–19.0 days postcoitum (d.p.c.). Viable *p107*^{-/-};*p130*^{-/-} embryos were present at a frequency consistent with Mendelian inheritance of the *p107* and *p130* null alleles (Table 1C), and no dead *p107*^{-/-};*p130*^{-/-} embryos were detected in utero. Hence, the absence of both p107 and p130 function was compatible with embryonic viability up to the time of birth but resulted in death at birth or shortly thereafter. From this, we concluded that p107 and p130 perform overlapping or redundant functions that are critical to postnatal mouse viability.

As one assessment of the postnatal development of mice of the eight surviving genotypes, weights of the progeny of *p107*^{+/-};*p130*^{+/-} mice were recorded approximately twice per week for 6 weeks. We found that *p107*^{-/-};*p130*^{+/-} mice were within the normal weight range at birth but attained only ~65% of the normal weight between 2 and 3 weeks of age (Fig. 3A). These mice died at increased frequency during the first and second weeks, and those that survived failed to reach the normal adult weight. These survivors also showed delayed fertility, and the females demonstrated reduced fertility. Because *p107*^{-/-};*p130*^{+/+} mice displayed none of these phenotypes, p130 appeared to be limiting in its ability to compensate for p107 loss in these *p107*^{-/-};*p130*^{+/-} mice. In contrast, p107 was able to compensate more fully for the loss of p130, as the *p107*^{+/-};*p130*^{-/-} mice exhibited only a modest and

transient growth delay from which they recovered at 3 weeks of age (Fig. 3A).

Numerous births were observed to evaluate the possible causes of death of *p107*^{-/-};*p130*^{-/-} neonates. In general, these neonates were born alive but had obvious breathing abnormalities and poor oxygenation that were apparent until they died at various times up to 6 hr later. Occasional *p107*^{-/-};*p130*^{-/-} neonates were not removed from their amniotic sacs by their mothers and either were born dead or died at least in part from maternal rejection. The breathing difficulties exhibited by live-born neonates may relate to morphological defects described below.

Morphology of p107^{-/-};*p130*^{-/-} embryos

Day 18.5 *p107*^{-/-};*p130*^{-/-} embryos had distinctive external features, including a moderately protruding abdomen, a shortened snout, and dramatically shortened limbs. Moreover, these embryos were up to 30% smaller than littermates (Fig. 3B). These characteristics first became obvious between embryonic days 15.0 and 16.0. Each of these phenotypes was also present in a mild form in *p107*^{-/-};*p130*^{+/-} embryos but not in embryos of other genotypes.

To characterize more precisely the limb development defect associated with combined *p107* and *p130* deficiency, a series of embryos were stained with dyes specific for cartilage (alcian blue) and bone (alizarin red); the soft tissue was then cleared with alkali. The resulting skeletal preparations revealed obvious aberrations in bone structure and in the timing of bone deposition in *p107*^{-/-};*p130*^{-/-} embryos.

As shown in Figure 4, 16.0 d.p.c. *p107*^{-/-};*p130*^{-/-} embryos had reduced rib cage size and dramatically reduced bone deposition in each of the long bones of the limbs (Fig. 4A–H). Most striking was the absence of bone deposition in the humerus in *p107*^{-/-};*p130*^{-/-} embryos compared to *p107*^{+/+};*p130*^{+/-} littermates (Fig. 4C,D). In contrast to their aberrant development of the ribs and long bones, which form through the process of endochondral ossification, most of the cranial bones of the *p107*^{-/-};*p130*^{-/-} embryos showed generally normal development (Fig. 4G,H); these bones form through intramembranous ossification. A notable exception in the cranium was provided by the interparietal bone, which forms at the posterior of the skull through endochondral ossification (Kaufman 1992). This bone was dramatically underdeveloped in 19.0 d.p.c. *p107*^{-/-};*p130*^{-/-} embryos (Fig. 4, I–L). A more subtle delay was also detected in the formation of the supraoccipital bone; this bone also forms by endochondral ossification. Together, these data indicated that p107 and p130 are needed for endochondral but not intramembranous bone development.

Combined *p107* and *p130* deficiency resulted not only in delayed ossification of long bones but also in their abnormal shape. The forelimbs of 19.0 day *p107*^{-/-};*p130*^{-/-} embryos did not resemble those of *p107*^{+/+};*p130*^{+/-} embryos at any point from 16.0 to 19.0 d.p.c.

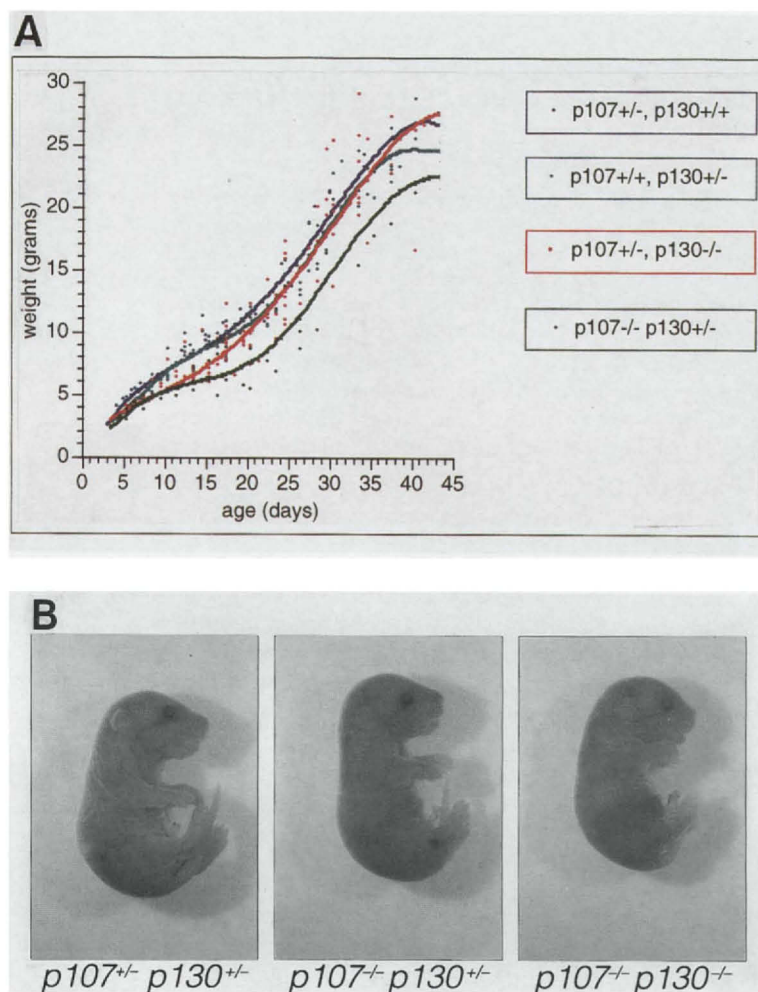


Figure 3. Analysis of mice and embryos with null alleles of *p107* and *p130*. (A) Postnatal growth. Weights were recorded approximately twice per week for mice of genotype *p107*^{+/-};*p130*^{+/+} (purple), *p107*^{+/-};*p130*^{+/-} (blue), *p107*^{+/-};*p130*^{-/-} (orange), and *p107*^{-/-};*p130*^{+/-} (green) over a 6-week period. Data points are indicated in the corresponding color. Biphasic growth curves were generated with a deltagraph curve fitting program. (B) External appearance of 18.5 d.p.c. *p107*^{+/-};*p130*^{+/-}, *p107*^{-/-};*p130*^{+/-}, and *p107*^{-/-};*p130*^{-/-} embryos.

and exhibited both shortening and thickening of the radius, ulna, and humerus (Fig. 5). Interestingly, *p107*^{-/-};*p130*^{+/-} embryos also had forelimb shortening and thickening consistent with their moderately shortened limbs visible in unstained embryos (see Fig. 3B). We also observed a subtle thickening of the radius, ulna, and humerus in *p107*^{-/-};*p130*^{+/+} embryos (Fig. 5). This is the first reproducible developmental anomaly attributable solely to the loss of p107 function. In contrast, forelimb development appears normal in *p107*^{+/-};*p130*^{-/-} and *p107*^{+/-};*p130*^{-/-} embryos (Fig. 5; data not shown).

Effect of p107 and p130 loss on chondrocyte proliferation in embryonic growth plates

Endochondral ossification is a well-characterized developmental process in which chondrocytes that form the cartilage of long bone epiphyses proliferate, become quiescent, hypertrophy, and finally are replaced by cancellous bone and marrow (Erlebacher et al. 1995). To determine precisely how endochondral ossification was impaired by combined p107 and p130 deficiency, a series of hematoxylin- and eosin-stained sections representing the centers of the epiphyseal growth plates of the humerus were prepared and analyzed.

General epiphyseal growth plate organization was retained in 18.0 d.p.c. *p107*^{-/-};*p130*^{-/-} embryos, with well-defined regions of flattened cells, hypertrophic cells, and cancellous bone (Fig. 6A). However, the growth plates were widened, the epiphyses were deformed and thickened, the zone of flattened cells was lengthened, the hypertrophic chondrocytes failed to form well-organized columns, and ossification of cancellous bone began at a greater-than-normal distance from the articular surface. Moreover, chondrocyte density in the epiphyseal centers was increased by approximately two-fold (Fig. 6A,B). In addition to these abnormalities in epiphyseal cartilage, aberrantly formed tracheal cartilage was also detected in some *p107*^{-/-};*p130*^{-/-} embryos (data not shown).

These observations suggested an abnormality in the proliferation of chondrocytes in certain cartilagenous settings. To examine the chondrocyte growth abnormality in epiphyseal cartilage more directly, 16.5 d.p.c. embryos were labeled with bromodeoxyuridine (BrdU) in utero for 1 hr prior to their collection; cells in S phase were then identified by immunostaining of the humerus with anti-BrdU antibody. Chondrocyte density in epiphyseal centers was increased in 16.5 d.p.c. *p107*^{-/-};*p130*^{-/-} embryos by ~30%. However, in these same

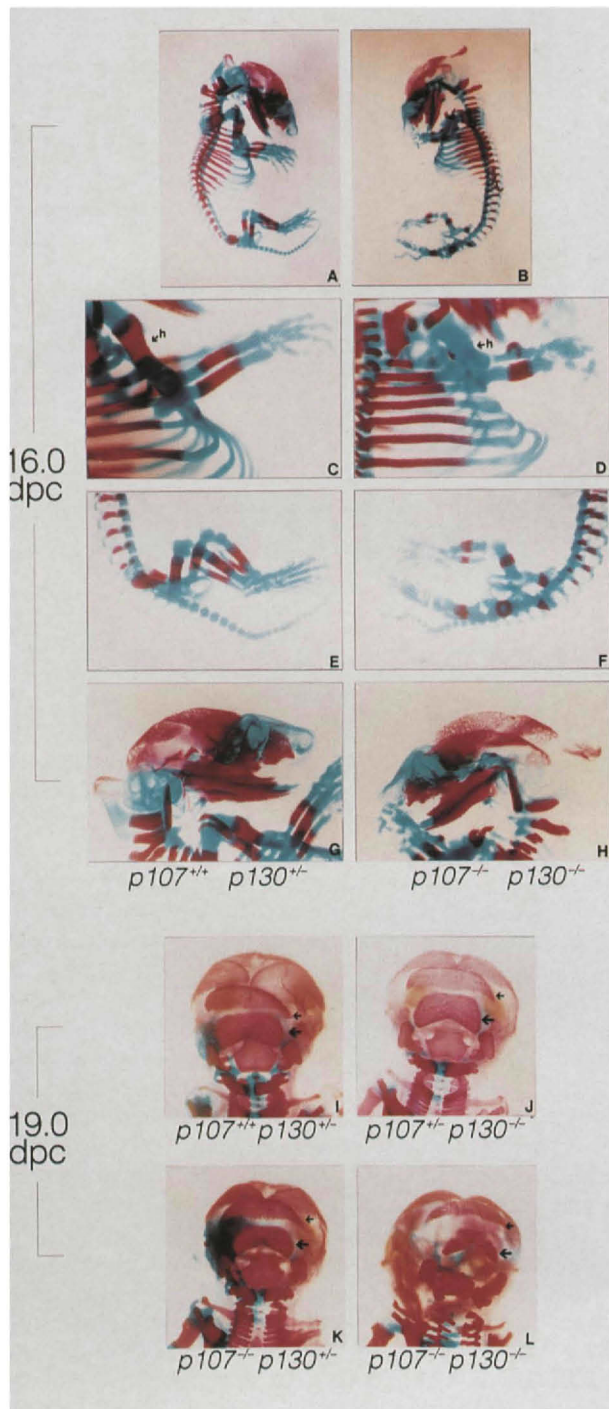


Figure 4. Effect of *p107* and *p130* gene loss on endochondral bone development. (A–H) Skeletal preparation of 16.0 d.p.c. $p107^{+/+}; p130^{+/+}$ (A,C,E,G) and $p107^{-/-}; p130^{-/-}$ (B,D,F,H) embryos stained with alcian blue and alizarin red. Note for $p107^{-/-}; p130^{-/-}$ embryos diminished rib cage size (A,B), diminished ossification of the long bones of the fore and hind limbs (C–F), including complete lack of ossification of the humerus (h), and generally normal ossification of the cranium (G,H). (I–L) Posterior view of skulls of 19.0 d.p.c. embryo skeletal preparations with genotypes as indicated. Note supraoccipital bone (short arrow) and smaller alizarin red-stained interparietal bone (long arrow) in $p107^{-/-}; p130^{-/-}$ embryo (L).

sections, we observed a striking two-fold increase in the proportion of chondrocytes that incorporated BrdU, from 11% of chondrocytes in $p107^{+/+}; p130^{+/+}$ embryos to 22% in $p107^{-/-}; p130^{-/-}$ littermates (Fig. 6C,D). The increase in BrdU labeling occurred primarily in epiphyseal centers, where chondrocytes are normally destined to enter a resting state later in development. The ability of chondrocytes to proliferate after exceeding the normal density at 16.5 d.p.c. explains the twofold higher density detected at 18.0 d.p.c. Increased BrdU labeling was less evident in the proliferation zone just below the epiphyseal head, where a high proportion of chondrocytes are normally found in the S phase of the cell cycle (Fig. 6D; data not shown).

The increase in chondrocyte proliferation in $p107^{-/-}; p130^{-/-}$ epiphyses indicated that p107 and p130 normally function to restrict chondrocyte growth within epiphyseal centers. Furthermore, the lengthening of the zone of flattened cells suggested that p107 and p130 also contribute to the chondrocyte cell cycle withdrawal and terminal differentiation that occurs in this region. However, p107 and p130 were not absolutely required for terminal differentiation in developing bone, as late steps in this process such as the expression of type X collagen, chondrocyte hypertrophy, and the replacement of hypertrophic cells with cancellous bone did occur in the absence of both p107 and p130 (Fig. 6A; data not shown).

The morphological defects observed here may be related to the deaths of $p107^{-/-}; p130^{-/-}$ neonates in several ways. In particular, the impaired rib development in $p107^{-/-}; p130^{-/-}$ neonates might have prevented sufficient lung expansion and inflation. Also, altered chondrocranial bone development of $p107^{-/-}; p130^{-/-}$ neonates may have caused compression of the cervical spinal canal and lethal apneas, as occurs in human infants with defective endochondral bone development (Pauli et al. 1984). Finally, defects detected in tracheal cartilage may have impaired airway function.

Discussion

The pRB-related p130 and p107 proteins have been implicated as having important roles in cell growth control. They are expressed in a wide variety of cell types, inhibit cell growth when ectopically expressed, and are bound and functionally inactivated by DNA tumor virus oncoproteins in a fashion that leads to cell transformation (Harlow et al. 1986; Whyte et al. 1988; Dyson et al. 1992; Cobrinik et al. 1993; Zhu et al. 1993; Claudio et al. 1994; Schneider et al. 1994; Christensen and Imperiale 1995; Vairo et al. 1995; Zalvide and DeCaprio 1995). Moreover, p130 and p107 bind and inhibit *trans*-activation by growth-promoting transcription factors including E2F-4, E2F-5, and (at least in the case of p107) the c-Myc protein (Zamanian and LaThangue 1993; Ginsberg et al. 1994; Gu et al. 1994; Beijersbergen et al. 1994a,b; Sardet et al. 1995; Vario et al. 1995). p130:E2F complexes are particularly prominent in cells that are in the G_0 state or that have undergone terminal differentiation, such as serum-starved mouse fibroblasts, resting T-lymphocytes, and

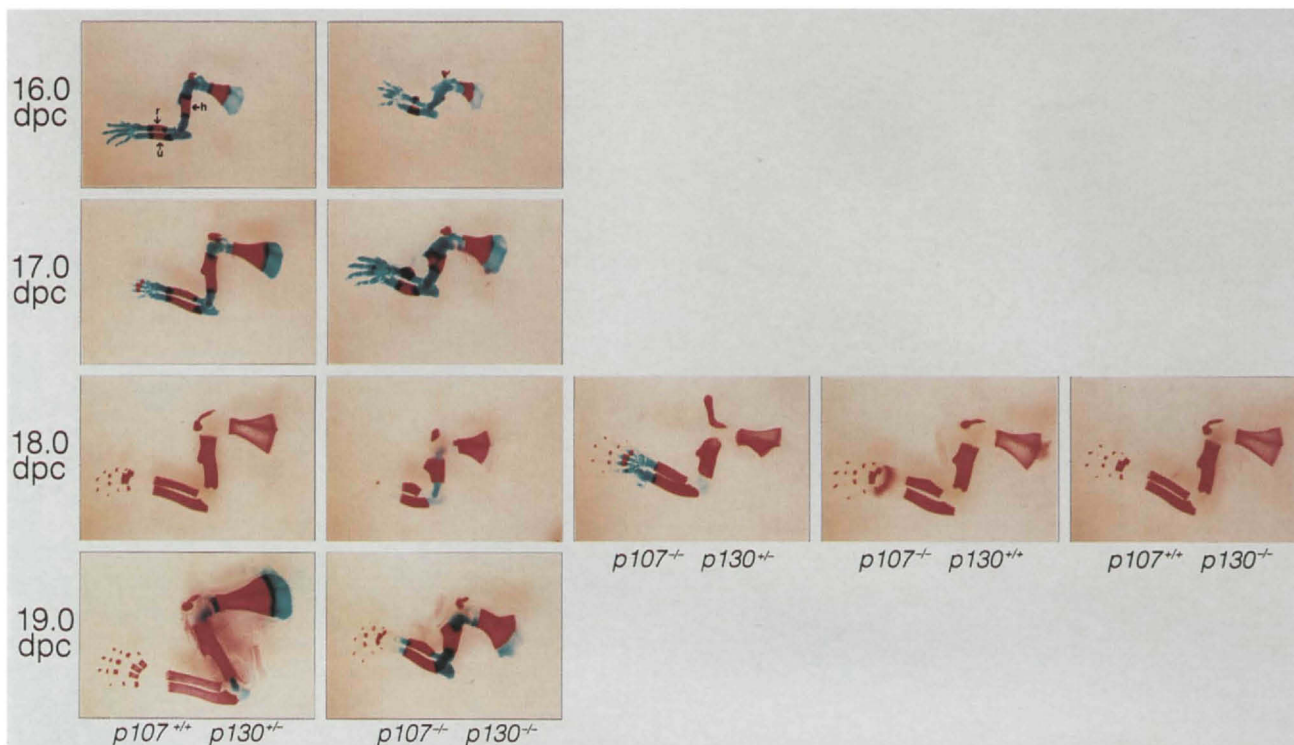


Figure 5. Effect of *p107* and *p130* loss on forelimb development. Alcian blue- and alizarin red-stained forelimbs prepared from 16.0–19.0 d.p.c. embryos, with genotypes as indicated. The humerus (h), radius (r), and ulna (u) are indicated in the top left panel.

differentiating muscle. *p107*:E2F complexes are present in various types of nonproliferating cells as well (Cobrinik et al. 1993; Shin et al. 1995; Vario et al. 1995). For these reasons, it seemed possible that *p130* and *p107* might widely contribute to the cell cycle withdrawal that accompanies cell differentiation and senescence.

Through the production of mice with null *p130* alleles, we have found that there is little developmental consequence associated with the absence of *p130*. In embryonic fibroblasts derived from such mice, *p107* largely compensated for the loss of *p130* in binding to E2F transcription factors, suggesting that *p107* may compensate more generally for *p130* loss. This view is supported by the developmental defect apparent in embryos that are deficient in both of these proteins.

p107^{-/-}; *p130*^{-/-} embryos exhibited increased chondrocyte density in epiphyseal cartilage, delayed and anomalous endochondral bone formation, and shortened limbs. These findings suggest that *p107* and *p130* con-

tribute to the orderly process of quiescence, hypertrophy, and replacement that is exhibited by chondrocytes during the process of endochondral bone development. In the absence of *p107/p130*-mediated control, chondrocytes in epiphyseal centers proliferate at an increased rate and reach a higher density, and chondrocytes in the zone of flattened cells experience a delay in the cell cycle withdrawal and hypertrophy that accompanies terminal differentiation. Significantly, chondrocytes eventually do cease proliferating in growth plates of *p107*^{-/-}; *p130*^{-/-} embryos, and we speculate that this is effected by other growth-inhibitory molecules that function in these cells such as pRB.

The growth of chondrocytes is likely to be governed by the coordinated actions of cdk. In many kinds of cells, cdk are required in the late G₁ phase of the cell cycle to phosphorylate pRB and thereby to release a rate-limiting pRB-imposed block to cell cycle progression (Weinberg 1995). Our results indicate that *p107* and *p130* impose

Figure 6. Effect of *p107* and *p130* loss on chondrocyte growth in long-bone epiphyses. (A) Hematoxylin- and eosin-stained distal humerus growth plates from 18.0 day *p107*^{+/+}; *p130*^{+/+} (top) and *p107*^{-/-}; *p130*^{-/-} (bottom) embryos. (a) Articular surface; (e) epiphysis; (f) zone of flattened cells; (h) zone of hypertrophic cells. Original magnification, 20×. (B) Relative chondrocyte density in humerus epiphyseal centers. Chondrocyte nuclei were counted from a defined area of hematoxylin- and eosin-stained 10- μ m sections in proximal (P) and distal (D) humerus epiphyseal centers of 18.0 d.p.c. embryos of the indicated genotypes, and the number was raised to the 3/2 power. Each bar represents counts from a single section. Error bars represent variation from independently localized epiphyseal centers. (C) Proximal humerus epiphyseal centers of 16.5 d.p.c. *p107*^{+/+}; *p130*^{+/+} (top) and *p107*^{-/-}; *p130*^{-/-} (bottom) embryos, immunostained with anti-BrdU antibody. Original magnification, 40×. (D) Relative chondrocyte density in proximal humerus epiphyseal centers (left) and percent BrdU-labeled nuclei in epiphyseal centers and proliferative zones (right) of 16.5 d.p.c. embryos. BrdU-labeled and unlabeled chondrocyte nuclei were counted from the photographs displayed in C.

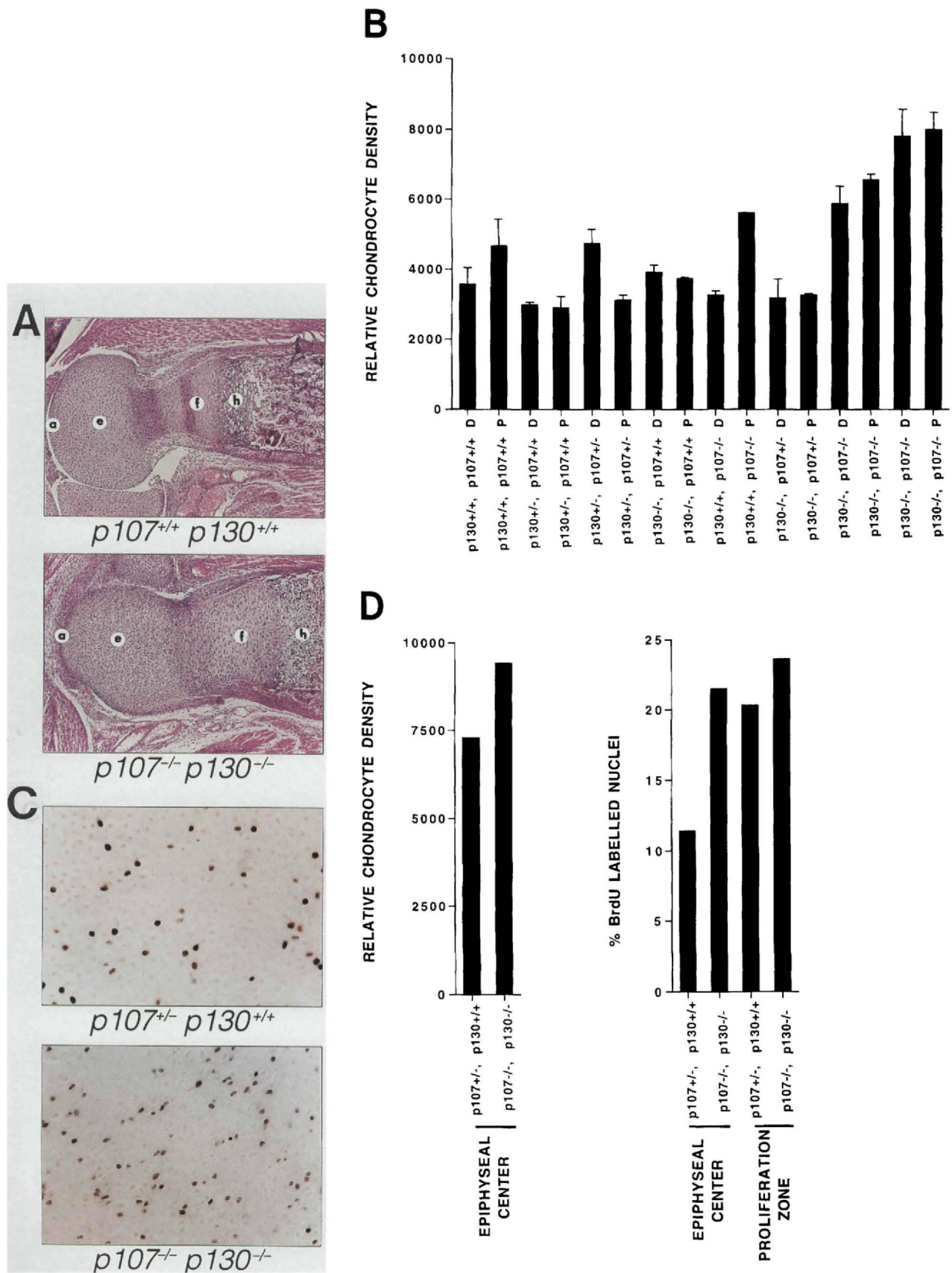


Figure 6. (See facing page for legend.)

control on cell cycle progression, most apparently, but not necessarily exclusively, in chondrocytes. In analogy to the growth control caused by pRB in other cell types, the p107/p130-imposed block is likely to be reversed in proliferating chondrocytes through the actions of cdk, particularly those of the cyclin D/cdk4 class that phosphorylate and thus functionally inactivate p107 and possibly p130 (Beijersbergen et al. 1995). The enhanced proliferation that we observed in p107- and p130-deficient chondrocytes suggests that signals that prevent p107 and p130 phosphorylation in long bone epiphyses are critical to the chondrocyte cell cycle withdrawal that occurs in this location.

Apart from their anomalous bone development, neonates deficient in both p107 and p130 appeared from histopathological analyses to be normal. Thus, the association of these proteins with E2Fs and the increase in p130 or p107 levels observed in terminally differentiated cells apparently is dispensable for differentiation and proliferation control processes in most tissues. In tissues that are not affected by p107 and p130 loss, pRB may control differentiation and proliferation sufficiently well to allow normal development. pRB is critical for normal growth control and for regulation of cyclin E expression in MEFs, despite the nearly undetectable levels of Rb:E2F complexes and high levels of p130:E2F complexes in such cells (Cobrinik et al. 1993; Herrera et al. 1996). These findings argue that pRB—even at low levels—may carry out critical growth control functions that cannot be performed by p107 and p130. In contrast, our results suggest that growth regulation by p107 and p130 can be substituted by pRB in tissues other than developing cartilage.

It remains possible, however, that p107 and p130 play critical cell growth-regulatory roles in other cell types in later postnatal life. In this regard, it will be interesting to see whether *p107^{+/-};p130^{-/-}* or *p107^{-/-};p130^{+/-}* mice develop tumors with loss of the remaining wild-type *p107* or *p130* allele.

The finding that developmentally significant growth regulation by p107 and p130 is largely restricted to chondrocytes suggests that these cells may be governed by unusual growth-regulatory programs. For example, chondrocytes may express low levels of pRB, thus requiring p107 and p130 to function as the rate-limiting inhibitors of proliferation. Alternatively, proteins regulated by pRB such as E2F-1, E2F-2, and E2F-3 (Lees et al. 1993), may not be expressed in chondrocytes, whereas growth-promoting proteins that are regulated by p107 or p130, such as E2F-4, E2F-5, and c-Myc (Ginsberg et al. 1994; Gu et al. 1994; Beijersbergen et al. 1994a,b; Sardet et al. 1995; Vairo et al. 1995), may have a more prominent role in chondrocytes than in other cell types.

Materials and methods

Production of p130 gene targeting vector, targeted ES cells, mice, and embryo fibroblasts

For construction of the *p130* targeting vector (pPNT-p130), a

16-kb genomic clone corresponding to a portion of the mouse *p130* locus was isolated using the human *p130* cDNA as a probe. An exon was located within the genomic clone by a combination of Southern blotting and sequence analysis. Using site-directed mutagenesis, an *EcoRV* site was generated within the exon at amino acid 108, numbering with reference to the human protein (Li et al. 1993). A genomic fragment extending 5' from this *EcoRV* site to a *SacI* site (4.5 kb total) was inserted into the disruption vector, pPNT (Tybulewicz et al. 1991), such that *p130* and *neo* were in opposite transcriptional orientations. A second fragment, derived from sequences 3' of the exon, extended 3.2 kb from a *Bam*HI site to a *Stu*I site. This was inserted into pPNT upstream of the *neo* transcription unit to form pPNT-p130.

pPNT-p130 was introduced into 129/Sv D3 ES cells as described (Gossler et al. 1986), and ES cells were selected for resistance to G418 and Gancyclovir (Mansour et al. 1988). DNA from selected clones was extracted, digested with *Bst*XI, and analyzed by Southern blotting using a ~340-bp PCR product (probe 1) generated with primers 5'-GAGTTTCCGGTCAGGAATACT and 5'-GGCCTCCAGTGGTTAAGA and corresponding to *p130* intron sequences located as in Figure 1A. DNA from clones with a 6.6-kb *Bst*XI fragment detected with this probe was digested with *EcoRV* and *Not*I and analyzed by Southern blotting using a ~130-bp PCR product (probe 2) generated with a primer, 5'-GCCACCCCGCGGCCCAAC-TCC, from *p130* genomic sequences and a vector primer, and corresponding to *p130* sequences located as in Figure 1A. Clones in which the pPNT-p130 targeting vector had undergone homologous recombination on both sides of the *neo* cassette (about one-third of the total) were injected into 3.5 day C57BL/6 blastocysts. Chimeric mice derived from these blastocysts were mated to C57BL/6 females, and the presence of the targeted *p130* allele was evaluated in agouti pups using Southern blotting as above or using PCR with the common primer 5'-ACG-GATGTCAGTGTACCG, the wild-type *p130*-specific primer 5'-TACATGGTTTCCTTCAGCGG, and the targeting vector-specific primer 5'-GAAGAACGAGATCAGCAG. Through use of Southern blotting we detected a polymorphism that gave rise to a 6.6-kb *Bst*XI fragment in wild-type C57BL/6 DNA detected with probe 1.

MEFs from progeny of a *p130^{+/-}* F₁ intercross were prepared, grown, serum-starved, and subjected to FACS analysis as described (Robertson 1987; Cobrinik et al. 1993). They were assayed for thymidine incorporation following a 1-hr incubation in 1 μ Ci/ml of [³H]-thymidine, a wash, and 30-min incubation in ice-cold 5% trichloroacetic acid, three washes in H₂O, lysis in 0.1N NaOH, and scintillation counting.

Protein analysis

MEF extract preparation, immunoprecipitations, and Western blotting were performed as described (Cobrinik et al. 1993). Gel mobility shifts utilized a 43-bp oligodeoxynucleotide probe corresponding to sequences in the c-Myc promoter as described (Cobrinik et al. 1993). p130 detection by immunoprecipitation, Western blot, and gel mobility shift utilized rabbit antiserum C-20, lot D134 from Santa Cruz Biotechnology. p107 was detected in gel mobility shift analyses using rabbit antiserum C-18 from Santa Cruz Biotechnology.

Embryo analysis

Embryonic bone and cartilage were stained with alcian blue and alizarin red as described (LeMouellic et al. 1992). For histologic

analysis, embryos were fixed in Bouin's solution (10% formaldehyde, 0.7% picric acid, 5% acetic acid) or neutral buffered formalin (3.7% formaldehyde, 45 mM Na₂HPO₄, 29 mM NaH₂PO₄) prior to preparation of 10- μ m sections. Embryos were labeled with BrdU by injecting pregnant females intraperitoneally with BrdU labeling reagent (Amersham) as recommended by the manufacturer. Sections either were stained with hematoxylin and eosin or were immunostained with anti-BrdU antibody as described (Morgenbesser et al. 1994) and counterstained with methyl green. Some sections were also stained with an anti-type X collagen antibody generously provided by Dr. Bjorn Olsen (Harvard Medical School, Boston, MA).

Acknowledgments

We thank J. Mkandawire and S. Matsumoto for technical assistance and B. Williams, A. Fazeli, S. Shi, L. Johnson, A. McClatchey, and K. McLeod for helpful discussions. D.C. was supported by a fellowship from the Susan G. Komen Breast Cancer Foundation. M.-H.L. was a recipient of an award from the Massachusetts General Hospital Fund for Medical Discovery. E.H. and R.A.W. are American Cancer Society research professors. T.J. is an Assistant Investigator and D.B. is an Investigator of the Howard Hughes Medical Institute. This work was supported by grants from the National Institutes of Health to N.D., E.H., D.B., R.A.W., and T.J.

The publication costs of this article were defrayed in part by payment of page charges. This article must therefore be hereby marked "advertisement" in accordance with 18 USC section 1734 solely to indicate this fact.

References

- Almasan, A., Y. Yin, R.E. Kelly, E.Y. Lee, A. Bradley, W. Li, J.R. Bertino, and G.M. Wahl. 1995. Deficiency of retinoblastoma protein leads to inappropriate S-phase entry, activation of E2F-responsive genes, and apoptosis. *Proc. Natl. Acad. Sci.* **92**: 5436–5440.
- Beijersbergen, R.L., E.M. Hijmans, L. Zhu, and R. Bernards. 1994a. Interactions of c-myc with the pRB-related protein p107 results in inhibition of c-myc-mediated transactivation. *EMBO J.* **13**: 4080–4086.
- Beijersbergen, R.L., R.M. Kerkhoven, L. Zhu, L. Carlee, P.M. Voorhoeve, and R. Bernards. 1994b. E2F-4, a new member of the E2F gene family, has oncogenic activity and associates with p107 in vivo. *Genes & Dev.* **8**: 2680–2690.
- Beijersbergen, R.L., L. Carlee, R.M. Kerkhoven, and R. Bernards. 1995. Regulation of the retinoblastoma protein-related p107 by G₁ cyclin complexes. *Genes & Dev.* **9**: 1340–1353.
- Christensen, J.B. and M.J. Imperiale. 1995. Inactivation of the retinoblastoma susceptibility protein is not sufficient for the transforming function of the conserved region 2-like domain of simian virus 40 large T antigen. *J. Virol.* **69**: 3945–3948.
- Clarke, A.R., E.R. Maandag, M. vanRoon, N.M.T. vanderLugt, M. vanderValk, M.L. Hooper, A. Berns, and H. teRiele. 1992. Requirement for a functional Rb-1 gene in murine development. *Nature* **359**: 328–330.
- Claudio, P.P., C.M. Howard, A. Baldi, A.D. Luca, Y. Fu, G. Condorelli, Y. Sun, N. Colburn, B. Calabretta, and A. Giordano. 1994. p130/pRb2 has growth suppressive properties similar to yet distinctive from those of retinoblastoma family members pRb and p107. *Cancer Res.* **54**: 5556–5560.
- Cobrinik, D., P. Whyte, D.S. Peeper, T. Jacks, and R.A. Weinberg. 1993. Cell cycle-specific association of E2F with the p130 E1A binding protein. *Genes & Dev.* **7**: 2392–2404.
- Dagnino, L., L. Zhu, K.L. Skorecki, and H.L. Moses. 1995. E2F-independent transcriptional repression by p107, a member of the retinoblastoma family of proteins. *Cell Growth & Diff.* **6**: 191–198.
- DeCaprio, J.A., J.W. Ludlow, J. Figge, J.-Y. Shew, C.-M. Huang, W.-H. Lee, E. Marsilio, E. Paucha, and D.M. Livingston. 1988. SV40 large tumor antigen forms a specific complex with the product of the retinoblastoma susceptibility gene. *Cell* **54**: 275–283.
- Dyson, N., P.M. Howley, K. Munger, and E. Harlow. 1989. The human papillomavirus-16 E7 oncoprotein is able to bind to the retinoblastoma gene product. *Science* **243**: 934–936.
- Dyson, N., P. Guida, K. Munger, and E. Harlow. 1992. Homologous sequences in adenovirus E1A and human papillomavirus E7 proteins mediate interaction with the same set of cellular proteins. *J. Virol.* **66**: 6893–6902.
- Erlebacher, A., E.H. Filvaroff, S.E. Gitelman, and R. Derynck. 1995. Toward a molecular understanding of skeletal development. *Cell* **80**: 371–378.
- Ewen, M.E., Y. Xing, J.B. Lawrence, and D.M. Livingston. 1991. Molecular cloning, chromosomal mapping, and expression of the cDNA for p107, a retinoblastoma gene product-related protein. *Cell* **66**: 1155–1164.
- Ewen, M.E., B. Faha, E. Harlow, and D. Livingston. 1992. Interaction of p107 with cyclin A independent of complex formation with viral oncoproteins. *Science* **255**: 85–87.
- Faha, B., M.E. Ewen, L.-H. Tsai, D.M. Livingston, and E. Harlow. 1992. Interaction between human cyclin A and adenovirus E1A-associated p107 protein. *Science* **255**: 87–90.
- Ginsberg, D., G. Vairo, T. Chittenden, Z.-X. Xiao, G. Xu, K.L. Wydner, J.A. DeCaprio, J.B. Lawrence, and D.M. Livingston. 1994. E2F-4, a new member of the E2F transcription factor family, interacts with p107. *Genes & Dev.* **8**: 2665–2679.
- Gossler, A., T. Doetschman, R. Korn, E. Serfling, and R. Kemler. 1986. Transgenesis by means of blastocyst-derived embryonic stem cell lines. *Proc. Natl. Acad. Sci.* **83**: 9065–9069.
- Gu, W., K. Bhatia, I.T. Magrath, C.V. Dang, and R. Dalla-Favera. 1994. Binding and suppression of the myc transcriptional activation domain by p107. *Science* **264**: 251–254.
- Hannon, G.J., D. Demetrick, D. Beach. 1993. Isolation of the Rb-related p130 through its interaction with CDK2 and cyclins. *Genes & Dev.* **7**: 2378–2391.
- Harlow, E., P. Whyte, B.J. Franza, and C. Schley. 1986. Association of adenovirus early-region 1A proteins with cellular polypeptides. *Mol. Cell. Biol.* **6**: 1579–1589.
- Herrera, R.E., V.P. Tan, B.O. Williams, T. Makela, R.A. Weinberg, and T. Jacks. 1996. Altered cell cycle kinetics, gene expression, and G1 restriction point regulation in Rb-deficient fibroblasts. *Mol. Cell. Biol.* **16**: 2402–2407.
- Hijmans, E.M., P.M. Voorhoeve, R.L. Beijersbergen, L.J.v.t. Veer, and R. Bernards. 1995. E2F-5, a new E2F family member that interacts with p130 in vivo. *Mol. Cell. Biol.* **15**: 3082–3089.
- Hoang, A.T., B. Lutterbach, B.C. Lewis, T. Yano, T.-Y. Chou, J.F. Barrett, M. Raffeld, S.R. Hann, and C.V. Dang. 1995. A link between increased transforming activity of lymphoma-derived MYC mutant alleles, their defective regulation by p107, and altered phosphorylation of the c-Myc transactivation domain. *Mol. Cell. Biol.* **15**: 4031–4042.
- Hu, Q., N. Dyson, and E. Harlow. 1990. The regions of the retinoblastoma protein needed for binding to adenovirus E1A or SV40 large T antigen are common sites for mutations. *EMBO J.* **9**: 1147–1155.
- Huang, H.-J.S., J.-K. Yee, J.-Y. Shew, P.-L. Chen, R. Bookstein, T. Friedman, E.Y.-H.P. Lee, and W.-H. Lee. 1988. Suppression

- of the neoplastic phenotype by replacement of the RB gene in human cancer cells. *Science* **242**: 1563–1566.
- Huang, S., N. Wang, B.Y. Tseng, W.-H. Lee, and E.Y.-H.P. Lee. 1990. Two distinct and frequently mutated regions of retinoblastoma protein are required for binding to SV40 T antigen. *EMBO J.* **9**: 1815–1822.
- Jacks, T., A. Fazeli, E.M. Schmitt, R.T. Bronson, M.A. Goodell, and R.A. Weinberg. 1992. Effects of an Rb mutation in the mouse. *Nature* **359**: 295–300.
- Kaelin, W.G., M.E. Ewen, and D.M. Livingston. 1990. Definition of the minimal simian virus 40 large T antigen- and adenovirus E1A-binding domain in the retinoblastoma gene product. *Mol. Cell. Biol.* **10**: 3761–3769.
- Kaufman, M. 1992. *The atlas of mouse development*. Academic Press, London, UK.
- Lee, E.Y.-H.P., C.-Y. Chang, N. Hu, Y.-C.J. Wang, C.-C. Lai, K. Herrup, W.-H. Lee, and A. Bradley. 1992. Mice deficient for Rb are nonviable and show defects in neurogenesis and hematopoiesis. *Nature* **359**: 288–294.
- Lee, M.-H., B.O. Williams, G. Mulligan, S. Mukai, R.T. Bronson, N. Dyson, E. Harlow, and T. Jacks. 1996. Targeted disruption of *p107*: Potential functional overlap between *p107* and *Rb*. (this issue).
- Lees, J., M. Saito, M. Vidal, M. Valentino, T. Look, E. Harlow, N. Dyson, and K. Helin. 1993. The retinoblastoma protein binds to a family of E2F transcription factors. *Mol. Cell. Biol.* **13**: 7813–7825.
- LeMouellic, H., F.Y. Lallemand, and P. Brulet. 1992. Homeosis in the mouse induced by a null mutation in the *hox-3.1* gene. *Cell* **69**: 251–264.
- Li, Y., C. Graham, S. Lacy, A.M.V. Duncan, and P. Whyte. 1993. The adenovirus E1A-associated 130-kD protein is encoded by a member of the retinoblastoma gene family and physically interacts with cyclins A and E. *Genes & Dev.* **7**: 2366–2377.
- Lukas, J., J. Bartkova, M. Rohde, M. Strauss, and J. Bartek. 1995. Cyclin D1 is dispensable for G1 control in retinoblastoma gene-deficient cells independently of *cdk4* activity. *Mol. Cell. Biol.* **15**: 6607–6615.
- Maandag, E.C., M. van der Valk, M. Vlaar, C. Feltkamp, J. O'Brein, M. vanRooy, N. van der Lugt, A. Berns, and H.T. Riele. 1994. Developmental rescue of an embryonic-lethal mutation in the retinoblastoma gene in chimeric mice. *EMBO J.* **13**: 4260–4268.
- Mansour, S.L., K.R. Thomas, and M.R. Capecchi. 1988. Disruption of the proto-oncogene *int-2* in mouse embryo-derived stem cells: A general strategy for targeting mutations to nonselectable genes. *Nature* **336**: 348–352.
- Mayol, X., X. Grana, A. Baldi, N. Sang, Q. Hu, and A. Giordano. 1993. Cloning of a new member of the retinoblastoma gene family (*pRb2*) which binds to the E1A transforming domain. *Oncogene* **8**: 2561–2566.
- Morgenbesser, S.D., B.O. Williams, T. Jacks, and R.A. DePinho. 1994. p53-dependent apoptosis produced by Rb-deficiency in the developing mouse lens. *Nature* **371**: 72–74.
- Pauli, R.M., C.I. Scott, E.R. Wassman, E.F. Gilbert, L.A. Leavitt, J. VerHoeve, J.G. Hall, M.W. Partington, K.L. Jones, A. Sommer, et al. 1984. Apnea and sudden unexpected death in infants with achondroplasia. *J. Pediatr.* **104**: 342–348.
- Robertson, E.J. 1987. Embryo-derived stem cell lines. In *Teratocarcinomas and embryonic stem cells: A practical approach*. [ed. E.J. Robertson], pp. 71–112. IRL Press, Oxford, UK.
- Sardet, C., M. Vidal, D. Cobrinik, Y. Geng, C. Onufryk, A. Chen, and R.A. Weinberg. 1995. E2F-4 and E2F-5, two novel members of the E2F family, are expressed in the early phases of the cell cycle. *Proc. Natl. Acad. Sci.* **92**: 2403–2407.
- Schneider, J.W., W. Gu, L. Zhu, V. Mahdavi, and B. Nadal-Ginard. 1994. Reversal of terminal differentiation mediated by p107 in Rb-/- muscle cells. *Science* **264**: 1467–1471.
- Shin, E.K., A. Shin, C. Paulding, B. Schaffhausen, and A.S. Yee. 1995. Multiple changes in E2F function and regulation occur upon muscle differentiation. *Mol. Cell. Biol.* **15**: 2252–2262.
- Slebos, A.J., M.H. Lee, B.S. Plunkett, T.D. Kessis, B.O. Williams, T. Jacks, L. Hedrik, M.B. Kastan, and K.A. Cho. 1994. p53-dependent G1 arrest involves pRB-related proteins and is disrupted by the human papillomavirus 16 E7 oncoprotein. *Proc. Natl. Acad. Sci.* **91**: 5320–5324.
- Smith, E.J. and J.R. Nevins. 1995. The Rb-related p107 protein can suppress E2F function independently of binding to cyclin A/cdk2. *Mol. Cell. Biol.* **15**: 338–344.
- Tybulewicz, V.L., C.E. Crawford, P.K. Jackson, R.T. Bronson, and R.C. Mulligan. 1991. Neonatal lethality and lymphopenia in mice with a homozygous disruption of the *c-abl* protooncogene. *Cell* **65**: 1153–1163.
- Vairo, G., D.M. Livingston, and D. Ginsberg. 1995. Functional interaction between E2F-4 and p130: Evidence for distinct mechanisms underlying growth suppression by different retinoblastoma protein family members. *Genes & Dev.* **9**: 869–881.
- Weinberg, R.A. 1995. The retinoblastoma protein and cell cycle control. *Cell* **81**: 323–330.
- Whyte, P., K.J. Buchkovich, J.M. Horowitz, S.H. Friend, M. Raybuck, R.A. Weinberg, and E. Harlow. 1988. Association between an oncogene and an anti-oncogene: The adenovirus E1A proteins bind to the retinoblastoma gene product. *Nature* **334**: 124–129.
- Williams, B.O., E.M. Schmitt, L. Remington, R.T. Bronson, D.M. Albert, R.A. Weinberg, and T. Jacks. 1994. Extensive contribution of Rb-deficient cells to adult chimeric mice with limited histopathological consequences. *EMBO J.* **13**: 4251–4259.
- Zalvide, J. and J.A. DeCaprio. 1995. Role of pRB-related proteins in simian virus 40 large-T-antigen-mediated transformation. *Mol. Cell. Biol.* **15**: 5800–5810.
- Zamanian, M. and N.B. LaThangue. 1993. Transcriptional repression by the Rb-related protein p107. *Mol. Biol. Cell* **4**: 389–396.
- Zhu, L., S. van den Heuvel, K. Helin, A. Fattaey, M. Ewen, D. Livingston, N. Dyson, and E. Harlow. 1993. Inhibition of cell proliferation by p107, a relative of the retinoblastoma protein. *Genes & Dev.* **7**: 1111–1125.
- Zhu, L., G. Enders, J.A. Lees, R.L. Beijersbergen, R. Bernards, and E. Harlow. 1995a. The pRB-related p107 contains two growth suppression domains: Independent interactions with E2F and cyclin/cdk complexes. *EMBO J.* **14**: 1904–1913.
- Zhu, L., E. Harlow, and B.D. Dynlacht. 1995b. p107 uses a p21^{CIP1}-related domain to bind cyclin/cdk2 and regulate interactions with E2F. *Genes & Dev.* **9**: 1740–1752.



Shared role of the pRB-related p130 and p107 proteins in limb development.

D Cobrinik, M H Lee, G Hannon, et al.

Genes Dev. 1996, **10**:

Access the most recent version at doi:[10.1101/gad.10.13.1633](https://doi.org/10.1101/gad.10.13.1633)

References

This article cites 54 articles, 33 of which can be accessed free at:
<http://genesdev.cshlp.org/content/10/13/1633.full.html#ref-list-1>

License

Email Alerting Service

Receive free email alerts when new articles cite this article - sign up in the box at the top right corner of the article or [click here](#).

